ments about comparison between experiment and theory cannot be made.

ACKNOWLEDGMENTS

It gives me pleasure to thank Professor L. M. Falicov for suggesting this problem and for his invaluable guidance and encouragement. This work has been directly supported by the National Science Foundation and the office of Naval Research. In addition, it has benefited from general support to the Material Sciences at the University of Chicago by the Advanced Research Projects Agency.

PHYSICAL REVIEW VOLUME 187, NUMBER 3 15 NOVEMBER 1969

Temperature-Dependent Knight Shift in Cadmium: A Theoretical Study

R. V. KASOWSKI*†

Department of Physics and James Franck Institute, The University of Chicago, Chicago, Illinois 60637

(Received 3 April 1969)

Experimentally the Knight shift in Cd is characterized by (1) an increase in the nuclear resonance frequency of more than 70% in the temperature range from 0 to 594°K (melting point), (2) an increase of 33% in the isotropic Knight shift at the melting point, and (3) an increase in the anisotropic Knight shift from a small negative value at $T=0$°K to a fairly large positive value at high temperatures. We find that this temperature dependence is theoretically accounted for by including the effects of lattice vibrations into the electronic structure which we have investigated by means of an empirical pseudopotential. The effect of the lattice vibrations is to decrease the strength of the pseudopotential. This makes the energy bands more free-electron-like, and the s character of the wave functions of the Fermi surface increases. It also destroys the cancellation of the contributions of the various p parts of the wave function to the anisotropic Knight shift, thus increasing the anisotropy as well. Many-body corrections were included by means of a temperature-independent enhancement factor and were determined empirically for $T=0$°K. The trend of the variation of the Knight shift with temperature, both isotropic and anisotropic, is explained.

I. INTRODUCTION

IN regard to its NMR properties, cadmium is not an ordinary metal. The variation of the resonance frequency with temperature T is more than eight times larger than that of any other metal.[1–4] Most metals exhibit a small fractional change in the isotropic Knight shift K_{iso} of generally less than 10% over the temperature range from 4°K to the melting point. In Cd, however, K_{iso} undergoes a fractional increase of about 70% in the temperature range from 4 to 594°K (melting point). Furthermore, upon melting, K_{iso} suffers an abrupt increase of 33%. Most metals show little change in K_{iso} at the melting point.

Cadmium is an hexagonal metal. Being noncubic, it exhibits an anisotropic Knight shift K_{an}.[5–7] The temperature dependence of K_{an} in Cd is also anomalous.[1–4] It starts from a small negative nonzero value at $T=0$°K, and after going through zero at a temperature between 0 and 60°K it increases to a fairly large value at the melting temperature.

The two results mentioned above seem to lead to a paradox. Since K_{iso} depends on the s part of the wave function, the first result seems to indicate that the wave function becomes more s-like as the temperature increases. The contribution to K_{an} depends mainly on the non-s character of the wave functions, mostly its p part. The fact that K_{an} increases with temperature would seem to indicate that the p character of the wave function also increases with temperature.

These temperature-dependent properties must somehow result from (1) the anisotropic expansion of the lattice with temperature and (2) the thermal lattice vibrations. Since the application of pressure to Cd does not reverse the large increase in either K_{iso} or K_{an},[8] the change in lattice parameters could not be a significant source of the anomalous temperature dependence.

The electronic properties of Cd at very low temperatures seems to be well accounted for. Stark and Falicov[9] (SF) have used de Haas–van Alphen (dHvA) data to fit an empirical nonlocal pseudopotential (PP). The Fermi surface resulting from this PP agrees to within a

* National Science Foundation Predoctoral Fellow. This work is being submitted as partial fulfillment for the requirements of the Ph.D. degree at the University of Chicago, Chicago, Ill.

† Present address: Central Research Dept. Experimental Station, E. I. DuPont de Nemours, Wilmington, Del.

[1] E. F. W. Seymor and G. A. Styles, Phys. Letters **10**, 269 (1964).

[2] F. Borsa and R. G. Barnes, J. Phys. Chem. Solids **27**, 567 (1966).

[3] S. N. Sharma and D. L. Williams, Phys. Letters **25A**, 738 (1967).

[4] R. G. Goodrich and S. A. Khan (to be published).

[5] A. Abragam, *The Principles of Nuclear Magnetism* (Oxford University Press, London, 1961).

[6] W. D. Knight, in *Solid State Physics*, edited by F. Seitz and D. Turnbull (Academic Press Inc., New York, 1956), Vol. II, p. 93.

[7] C. P. Slichter, *Principles of Magnetic Resonance* (Harper and Row Publishers, Inc., New York, 1963).

[8] T. Kushida and L. Rimai, Phys. Rev. **143**, 157 (1966).

[9] R. W. Stark and L. M. Falicov, Phys. Rev. Letters **19**, 795 (1967); and unpublished.

few percent with all reported extremal cross-sectional areas as measured by the dHvA effect and even gives the correct compensation of electrons and holes in the bands to an accuracy of 3×10^{-4} electrons per atom. The noteworthy feature is that a nonlocal PP was necessary to fit the dHvA data and that the resultant Fermi surface is appreciably different from what one expects for a hexagonal-close-packed (hcp) nearly-free-electron metal.

This PP has already proved successful on two other different fronts: (1) The predicted Fermi surface agrees excellently with detailed radio-frequency size-effect measurements,[10] and (2) the phonon mass enhancement and density of states at the Fermi energy agree well with those extracted from superconductivity experiments.[11] In fact, this PP should accurately predict any low-temperature electronic properties (such as transport phenomena and the Knight shift) which depend on the electronic states at the Fermi surface.

In this paper, we incorporate temperature effects, such as lattice vibrations and thermal expansion, into the PP of SF and then calculate $K_{\rm iso}$, $K_{\rm an}$, and the spin susceptibility χ_p as a function of temperature. We find good agreement with experiment.

Section II contains the formulation of the theory. The thermal effects are incorporated into the one-electron Hamiltonian in Sec. III with the resulting temperature-dependent Fermi surface presented in Sec. IV. Section V is devoted to a calculation of the spin susceptibility and Knight shift. Section VI contains the conclusions and discussion.

II. KNIGHT-SHIFT FORMULATION

The Knight shift is a result of the interaction of the spin $\mathbf{s}$ and orbital angular momentum $\mathbf{l}$ of the conduction electrons with the spin $\mathbf{I}$ of the nucleus. The Hamiltonian[5] for the interaction of a given nuclear spin (jth) with the conduction electrons is

$$\hat{H}_{enj}=\gamma_e\gamma_n\hbar^2\mathbf{I}\cdot\sum_l\left(\frac{8\pi}{3}\mathbf{s}\delta(\mathbf{r}_{lj})+\frac{3\mathbf{r}_{lj}(\mathbf{s}_l\cdot\mathbf{r}_{lj})-\mathbf{s}_l r_{lj}^2}{r_{lj}^5}+\frac{\mathbf{l}}{r_{lj}^3}\right), \quad (2.1)$$

where $\mathbf{r}_{lj}=\mathbf{r}_l-\mathbf{R}_j$ and $\mathbf{r}_l$ is the position of the lth electron, $\mathbf{R}_j$ is the jth nucleus's position, and γ_l and γ_n are the gyromagnetic ratios of the electron and nucleus, respectively.

The Hamiltonian $\hat{H}_{enj}$ is weak compared to that for the electrons and is treated by perturbation theory in terms of the states of the electrons and nuclear spins.

Generally the isotropic Knight shift[6,7] is considered to be a result of only the hyperfine contact interaction and is given by

$$K_{\rm iso}=\Delta H/H=(8\pi/3)\chi_p\langle|\psi_{\rm k}(0)|^2\rangle_F, \quad (2.2)$$

where χ_p is the Pauli spin susceptibility and $\langle|\psi_{\rm k}(0)|^2\rangle_F$ is a measure of the electronic density of conduction electrons at the nuclear site averaged over the Fermi surface.

However, polarization of the core electrons can also contribute to $K_{\rm iso}$. The spin polarization of the conduction electrons causes the spin-up and spin-down core electrons to experience a different exchange force. As a result, the spatial part of the two wave functions of the core states for the two spins are different, and there is a slight imbalance of core-electron spin density at the nucleus. This core polarization contributes to $K_{\rm iso}$ through the contact term. No proof exists as to the sign of the core-polarization contribution to $K_{\rm iso}$.[12]

The second term in the Hamiltonian, the spin dipolar interaction, produces a shift of the nuclear resonance which depends on the orientation of the external field with respect to the crystal axis.[13] This anisotropy is zero for cubic crystals. For noncubic crystals the calculation of $K_{\rm an}$ involves calculating the diagonal matrix elements of the Legrendre polynomial $P_2(\cos\alpha)$, where α is the angle between the external magnetic field $\mathbf{H}_0$ and the radius vector $\mathbf{r}$ from the nuclear position to the electron.

To a good approximation, the electron wave function around a given lattice site can be thought of as a linear combination of parts with s symmetry, p symmetry, and d symmetry only. The nonvanishing matrix elements of $P_2(\cos\alpha)$ are thus only p-p and s-d matrix elements. The p symmetry usually makes the dominant contribution.

For an hcp crystal like Cd, the anisotropic contribution to the Knight shift[13] can be written in terms of a shift parallel to the hexagonal axis and a shift perpendicular to it,

$$K_{\parallel}=K_{\rm iso}+2\chi_p q_F, \quad K_{\perp}=K_{\rm iso}-\chi_p q_F,$$

where

$$q_F=\left\langle\int\psi_{\rm k}^*\frac{3z^2-r^2}{r^5}\psi_{\rm k}d^3\mathbf{r}\right\rangle_F$$

and $\langle\ \rangle_F$ indicates, once again, an average over the Fermi surface.

The quantity q_F serves to indicate the anisotropy (within a unit cell) of the electronic charge of states at the Fermi energy. The usual expression for the anisotropic Knight shift is

$$K_{\rm an}=K_{\parallel}-K_{\perp}=3\chi_p q_F. \quad (2.3)$$

The last term in H_{enj} is the orbital hyperfine term and contributes to $K_{\rm iso}$ via an orbital paramagnetism.

[10] R. C. Jones, R. G. Goodrich, and L. M. Falicov, Phys. Rev. **174**, 672 (1968).

[11] P. B. Allen, M. L. Cohen, L. M. Falicov, and R. V. Kasowski, Phys. Rev. Letters **21**, 1794 (1968).

[12] M. H. Cohen, D. A. Goodings, and V. Heine, Proc. Phys. Soc. (London) **73**, 811 (1959); G. D. Gaspari, W.-M. Shyu, and T. P. Das, Phys. Rev. **134**, A852 (1964); W.-M. Shyu, T. P. Das, and G. D. Gaspari, *ibid.* **152**, 270 (1966); P. Jena, S. D. Mahanti, and T. P. Das, Phys. Rev. Letters **20**, 544 (1968).

[13] N. Bloembergen and T. J. Rowland, Acta Met. **1**, 731 (1953); T. J. Rowland, Progr. Mater. Sci. **9**, 1 (1961).

A quantitative estimate of the orbital contribution from first principles is difficult.[14]

We simplify our calculation of the Knight shift by assuming that core-polarization and orbital effects can be neglected. The justification of this assumption is found in the recent spin-lattice relaxation-time measurements for Cd of Dickson.[15] Dickson finds that relaxation-time measurements indicate that the contribution of both core-polarization and orbital effects to $K_{\rm iso}$ in Cd is less than 10% of the contact interaction term and is of opposite sign.

In summary, we assume in this paper that $K_{\rm iso}$ is a direct result of the hyperfine contact interaction, and $K_{\rm an}$ derives solely from the spin-dipolar interaction.

III. THERMAL EFFECTS IN LOW-TEMPERATURE BAND STRUCTURES

A. Introduction

Most energy-band calculations, which are based on a one-electron theory, are done in the approximation that the nuclei are at rest and at their equilibrium positions. This approximation is valid at $T=0$°K for nuclei which have a negligible zero-point motion. However, as the temperature is increased, thermal lattice vibrations are excited and the nuclei undergo displacements about their equilibrium positions. These displacements can be analyzed in terms of the normal phonon modes of the solid.

To obtain the possible electron energies and wave functions at all temperatures, we need to incorporate the thermal vibrations into the Hamiltonian for the electron system.

The two contributions to the temperature dependence of the electronic properties of the system are (1) the implicit effect of the volume thermal expansion of the solid, and (2) the explicit effect of the electron-phonon interactions in the crystal at constant volume.

In this section, we will treat the temperature dependence of the electronic energies and wave functions (resulting from the thermal vibrations) in the Born-Oppenheimer approximation and then set up the formalism to do a practical calculation of the energy levels of cadmium as a function of temperature. The $T=0$°K PP of SF will be the starting point.

B. Schrödinger Equation for Electrons

Thermal effects cause the ions to suffer displacements about their equilibrium positions. Let us denote the instantaneous position of the νth atom by $\mathbf{R}_\nu$; a lattice configuration is then specified by the set $\{\mathbf{R}_\nu\}$ of ion positions. The Born-Oppenheimer (BO) approximation[16] allows one to write the Schrödinger equation for the electrons in a static lattice, the particular ion configuration being specified by $\{\mathbf{R}_\nu\}$, as

$$\left(\sum_i \frac{-\hbar^2}{2m}\frac{\partial^2}{\partial \mathbf{r}_i}+\sum_{ij}{}' \frac{e^2}{|\mathbf{r}_i-\mathbf{r}_j|}+V(\{\mathbf{R}_\nu\},\{\mathbf{r}_i\})\right) \times\psi_n(\{\mathbf{R}_\nu\},\{\mathbf{r}_i\})=E_n(\{\mathbf{R}_\nu\})\psi_n(\{\mathbf{R}_\nu\},\{\mathbf{r}_i\}), \quad (3.1)$$

where $\psi_n(\{\mathbf{R}_\nu\},\{\mathbf{r}_i\})$ is a many-electron wave function and the terms in the Hamiltonian are the electron kinetic energy, the electron-electron interaction, and the potential energy of the electrons in the field of the ions (in their displaced positions $\{\mathbf{R}_\nu\}$), respectively.

The lattice dynamical equation (in the BO approximation) which gives the normal phonon modes is

$$\left(\sum_\nu -\frac{\hbar^2}{2M}\frac{\partial^2}{\partial \mathbf{R}_\nu^2}+U(\{R_\nu\})+\langle E_n(\{\mathbf{R}_\nu\})\rangle_e\right)\chi_j(\{\mathbf{R}_\nu\}) =(E_T)_j\chi_j(\{\mathbf{R}_\nu\}), \quad (3.2)$$

where $\langle\ \rangle_e$ refers to a thermal average over the many-electron states.

The Schrödinger equation (3.1) for the electrons depends on the exact nuclear configuration. However, measurements of electron energies and other physical quantities depend only on the average configuration of the nuclei. Therefore we must calculate the ensemble average of the expectation value of operators which depend on the lattice positions. This average is taken by analyzing the nuclear displacements in terms of phonons and taking the average thermal occupation of all phonon states.

In what follows, the electrons are treated in the one-electron approximation; this means that the electron-electron interaction is approximated by a self-consistent (Hartree) field. We are interested in calculating ensemble averages of one-electron energies

$$\langle E_{\rm k}(\{\mathbf{R}_\nu\})\rangle_P=\langle\chi_j(\{\mathbf{R}_\nu\})|(\psi_{\rm k}(\mathbf{r},\{\mathbf{R}_\nu\}),[T+V(\mathbf{r},\{\mathbf{R}_\nu\})] \times\psi_{\rm k}(\mathbf{r},\{\mathbf{R}_\nu\}))|\chi_j(\{\mathbf{R}_\nu\})\rangle_P, \quad (3.3)$$

where $\langle\ \rangle_P$ denotes the phonon ensemble average, $\psi_{\rm k}(\mathbf{r},\{\mathbf{R}_\nu\})$ is a given one-electron wave function, and $E_{\rm k}(\{\mathbf{R}_\nu\})$ is the one-electron energy for the state $\mathbf{k}$[17] for a particular configuration $\{\mathbf{R}_\nu\}$. $V(\mathbf{r},\{\mathbf{R}_\nu\})$ is the self-consistent potential seen by the electron.

The calculation of $\langle E_{\rm k}(\{\mathbf{R}_\nu\})\rangle_P$ can be further simplified by using the PP method to solve for the electron states. A simple derivation of a PP formalism[18] based on the orthogonality of the core and conduction-electron wave functions will be briefly discussed here.

The electron wave function can be written in the form

$$\psi_{\rm k}(\mathbf{r},\{\mathbf{R}_\nu\})=\phi_{\rm k}(\mathbf{r})-\sum_{tj}\Theta_t(\mathbf{r}-\mathbf{R}_j)\langle\Theta_t(\mathbf{r}-\mathbf{R}_j)|\phi_{\rm k}\rangle, \quad \phi_{\rm k}(\mathbf{r})=\sum\alpha_{\mathbf{G}+\mathbf{k}}|\mathbf{G}+\mathbf{k}\rangle, \quad (3.4)$$

[14] R. J. Noer and W. D. Knight, Rev. Mod. Phys. **36**, 177 (1964).

[15] E. M. Dickson, thesis, University of California, Berkeley, 1968 (unpublished); Phys. Rev. **184**, 294 (1969).

[16] J. M. Ziman, *Theory of Solids* (Cambridge University Press, New York, 1964).

[17] k indicates all the necessary quantum numbers which define the state, but it is not necessarily a wave vector.

[18] W. A. Harrison, *Pseudopotentials in the Theory of Metals* (W. A. Benjamin, Inc., New York, 1966).

where $\Theta_t(\mathbf{r}-\mathbf{R}_j)$ are the core states with quantum numbers t centered at the ion positions $\mathbf{R}_j$, and $\mathbf{G}$ is a reciprocal-lattice vector; $|\mathbf{G}+\mathbf{k}\rangle$ denotes a normalized plane wave with wave vector $\mathbf{G}+\mathbf{k}$.

The one-electron wave equation, with the use of (3.4), becomes

$$(T+V+V_R)\phi_\mathbf{k}=E_\mathbf{k}\phi_\mathbf{k},$$

where

$$V_R\phi_\mathbf{k}=\sum_{tj}(E_\mathbf{k}-E_t)\Theta_t(\mathbf{r}-\mathbf{R}_j)\langle\Theta_t|\phi_\mathbf{k}\rangle.$$

The operator V_R has the character of a repulsive potential which cancels out most of $V(\mathbf{r},\{\mathbf{R}_\nu\})$. One can think of the electron as moving in a smooth PP $V_{\text{eff}}=V+V_R$, with pseudo-wave-function ϕ_k.

Equation (3.3) for the one-electron energy becomes equivalent to the simpler pseudo-wave-equation

$$\langle E_\mathbf{k}(\{\mathbf{R}_\nu\})\rangle_P=\langle\chi_j(\{\mathbf{R}_\nu\})|(\phi_\mathbf{k}(\mathbf{r},\{\mathbf{R}_\nu\}),[T+V_{\text{eff}}(\mathbf{r},\{\mathbf{R}_\nu\})]\phi_\mathbf{k}(\mathbf{r},\{\mathbf{R}_\nu\}))|\chi_j(\{\mathbf{R}_\nu\})\rangle_P. \quad (3.5)$$

Since V_{eff} is small, it is possible to use perturbation theory to calculate the instantaneous one-electron energy and wave function. In the nondegenerate case we have

$$\begin{aligned}E_\mathbf{k}(\{\mathbf{R}_\nu\})&=E_\mathbf{k}^0+\langle\mathbf{k}|V_{\text{eff}}|\mathbf{k}\rangle+\sum_{\mathbf{k}'}{}'\frac{|\langle\mathbf{k}|V_{\text{eff}}|\mathbf{k}'\rangle|^2}{(E_\mathbf{k}^0-E_{\mathbf{k}'}^0)},\\ \phi_\mathbf{k}'(\mathbf{r}\{\mathbf{R}_\nu\})&=|\mathbf{k}\rangle+\sum_{\mathbf{k}'}{}'\frac{\langle\mathbf{k}'|V_{\text{eff}}|\mathbf{k}\rangle}{(E_\mathbf{k}^0-E_{\mathbf{k}'}^0)}|\mathbf{k}'\rangle,\end{aligned} \quad (3.6)$$

where $E_\mathbf{k}^0$ and $|\mathbf{k}\rangle$ are the free-electron energy and wave function, respectively.

Calculation of $\langle E_\mathbf{k}(\{\mathbf{R}_\nu\})\rangle_P$ thereby reduces to the task of calculating the ensemble average of both the Fourier coefficients of the effective potential V_{eff} and their absolute values squared.

We now make the rigid-ion approximation in which we assume V_{eff} to be a sum of ionic potentials, whose shape is independent of the ionic position:

$$V_{\text{eff}}=\sum_\nu v_{\text{eff}}(\mathbf{r}-\mathbf{R}_\nu).$$

The Fourier coefficients and their absolute value squared then become

$$\begin{aligned}&\langle\langle\mathbf{k}'|V_{\text{eff}}|\mathbf{k}\rangle\rangle_P\\ &\quad=(dN)^{-1}(\mathbf{k}',v_{\text{eff}}\mathbf{k})\langle\sum_\nu e^{i(\mathbf{k}-\mathbf{k}')\cdot(\mathbf{R}_\nu^0+\mathbf{y}_\nu)}\rangle_P,\\ &\langle|\langle\mathbf{k}'|V_{\text{eff}}|\mathbf{k}\rangle|^2\rangle_P\\ &\quad=(dN)^{-2}\sum_{\mu\nu}e^{i(\mathbf{k}-\mathbf{k}')\cdot(\mathbf{R}_\nu^0-\mathbf{R}_\mu^0)}|(\mathbf{k}',v_{\text{eff}}\mathbf{k})|^2\\ &\qquad\times\langle e^{i(\mathbf{k}-\mathbf{k}')\cdot(\mathbf{y}_\nu-\mathbf{y}_\mu)}\rangle_P,\end{aligned} \quad (3.7)$$

where N is the number of unit cells in the crystal, $\mathbf{R}_\nu^0$ is the equilibrium position of the νth atom, $\mathbf{y}_\nu$ is the displacement from equilibrium, d is the number of atoms per unit cell, and

$$(\mathbf{k}',v_{\text{eff}}\mathbf{k})=\frac{1}{V_0}\int d\mathbf{r}\,e^{-i\mathbf{k}'\cdot\mathbf{r}}v_{\text{eff}}(\mathbf{r})e^{i\mathbf{k}\cdot\mathbf{r}},$$

with V_0 being the volume per atom.

The ion displacement $\mathbf{y}_\nu$ is expanded in terms of the normal phonon modes[19]:

$$\mathbf{y}_\nu=\sum_{qs}(\hbar/2MN\omega_{qs})^{1/2}(\mathbf{e}_{qsb}a_{qs}e^{i\mathbf{q}\cdot\mathbf{R}_\nu^0}+\mathbf{e}_{qsb}a_{qs}^+e^{i\mathbf{q}\cdot\mathbf{R}_\nu^0}). \quad (3.8)$$

In (3.8), a_{qs} and a_{qs}^+ are the destruction and creation operators for phonons in the mode $\mathbf{q}s$, e_{qsb} is a polarization vector, the index b labels the atoms in a unit cell, and $\mathbf{R}_\nu^0=\mathbf{R}_l^0+\mathbf{R}_b^0$, where $\mathbf{R}_b^0$ is the equilibrium position of the bth atom within the lth unit cell.

For a general process where no real phonons are created or destroyed, it has been proved by Glauber[20] that

$$\langle e^{i\mathbf{k}\cdot\mathbf{y}_\nu}\rangle_P=e^{-W},$$

where

$$W=\tfrac{1}{2}\sum_{qs}(\hbar/2MN\omega_{qs})(2\bar{n}_{qs}+1)|\mathbf{k}\cdot\mathbf{e}_{qsb}|^2 \quad (3.9)$$

and $\bar{n}_{qs}$ is the average occupation number of phonons in the mode $\mathbf{q}s$. (The usual Debye-Waller factor is e^{-2W}).

Using (3.9), the ensemble average of the Fourier coefficient (3.7) becomes

$$\langle\langle\mathbf{k}'|V_{\text{eff}}|\mathbf{k}\rangle\rangle_P=(\mathbf{k}',v_{\text{eff}}\mathbf{k})\frac{1}{d}\sum_b e^{i\mathbf{G}\cdot\mathbf{R}_b^0}\times e^{-W(\mathbf{G},T)}\delta_{\mathbf{k}-\mathbf{k}',\mathbf{G}}. \quad (3.10)$$

In the Appendix we prove that the Fourier coefficient squared is

$$\begin{aligned}\langle|\langle\mathbf{k}'V_{\text{eff}}|\mathbf{k}\rangle|^2\rangle_P=&|(\mathbf{k}',v_{\text{eff}}\mathbf{k})d^{-1}\\ &\times\sum_b e^{i\mathbf{G}\cdot\mathbf{R}_b^0}e^{-W(\mathbf{G},T)}|^2\delta_{\mathbf{k}-\mathbf{k}',\mathbf{G}}+(\hbar/2MN\omega_{qs})\\ &\times|\sum_b(\mathbf{k}-\mathbf{k}')\cdot e_{qsb}d^{-1}e^{i\mathbf{G}\cdot\mathbf{R}_b^0}e^{-W}(\mathbf{k}',v_{\text{eff}}\mathbf{k})|^2\\ &\times(2\bar{n}_{qs}+1)\delta_{\mathbf{k}-\mathbf{k}'\pm\mathbf{q},\mathbf{G}}.\end{aligned} \quad (3.11)$$

The second term is an electron-phonon interaction or self-energy contribution to $\langle E_\mathbf{k}\rangle_P$. This term is of negligible importance compared to the first term and is omitted.[21]

[19] J. M. Ziman, *Electrons and Phonons* (Oxford University Press, London, 1960).

[20] R. J. Glauber, Phys. Rev. **84**, 395 (1965); **98**, 1692 (1955).

[21] We have calculated it for a typical case, and it is less than 10% of the dominant term.

Then we have

$$\langle E_{\mathbf{k}}(\{\mathbf{R}_\nu\})\rangle_P = E_{\mathbf{k}}^0 + (\mathbf{k}', v_{\text{eff}}\mathbf{k}) d^{-1} \times \sum_b e^{i\mathbf{G}\cdot\mathbf{R}_b^0} e^{-W} \delta_{\mathbf{k}-\mathbf{k}',\mathbf{G}} + \sum_{\mathbf{k}'}{}' (E_{\mathbf{k}}^0 - E_{\mathbf{k}'}^0)^{-1} |(\mathbf{k}', v_{\text{eff}}\mathbf{k}) d^{-1} \times \sum_b e^{i\mathbf{G}\cdot\mathbf{R}_b^0} e^{-W}|^2 \delta_{\mathbf{k}-\mathbf{k}',\mathbf{G}}. \quad (3.12)$$

Note that by neglecting the second term in (3.11), we have regained periodicity. Consequently, the electron can be thought of as moving in a periodic effective potential $\langle V_{\text{eff}}(\mathbf{r},\{\mathbf{R}_\nu\})\rangle_P$ with a wave function $\bar{\phi}_{\mathbf{k}}$ which satisfies the equations

$$(T + \langle V_{\text{eff}}(\mathbf{r},\{\mathbf{R}_\nu\})\rangle_P)\bar{\phi}_{\mathbf{k}} = \langle E_{\mathbf{k}}(\{\mathbf{R}_\nu\})\rangle_P \bar{\phi}_{\mathbf{k}}, \quad (3.13)$$

$$\bar{\phi}_{\mathbf{k}} = \phi_{\mathbf{k}} + \sum_{\mathbf{k}'}{}' \frac{\langle \phi_{\mathbf{k}'} | \langle V_{\text{eff}}\rangle_P | \phi_{\mathbf{k}}\rangle}{E_{\mathbf{k}}^0 - E_{\mathbf{k}'}^0} \phi_{\mathbf{k}'}. \quad (3.14)$$

We refer to $\bar{\phi}_{\mathbf{k}}$ as the ensemble average pseudo-wave-function.

The results above justify our speaking of a Brillouin zone and Fermi surface for other than $T=0°\text{K}$.

C. Formulation of Knight-Shift Temperature Dependence

Now we would like to relate the ensemble average pseudo-wave-function $\bar{\phi}_{\mathbf{k}}$ of (3.14) to the calculation of the Knight shift.

The hyperfine interaction between the electrons and the jth nucleus depends on the nuclear configuration $\{\mathbf{R}_\nu\}$. We are interested in the ensemble average of this nuclear-electronic coupling

$$\langle \hat{H}_{enj}\rangle_P = \sum_l -(8\pi/3)\gamma_l\gamma_n \langle\langle \Psi_e(\{\mathbf{r}_i\},\{\mathbf{R}_\nu\})| \times \mathbf{I}_j\cdot\mathbf{s}_l\delta(\mathbf{r}-\mathbf{R}_j)|\Psi_e(\{\mathbf{r}_i\},\{\mathbf{R}_\nu\})\rangle\rangle_P, \quad (3.15)$$

where Ψ_e is the many-electron wave function.

The wave function Ψ_e is a product of one-electron wave functions $\psi_{\mathbf{k}}$ properly antisymmetrized to take account of the Pauli exclusion principle. Using this Ψ_e we obtain

$$\langle \hat{H}_{enj}\rangle_P = (8\pi/3)\gamma_l\gamma_n I_{zj} \sum_{\mathbf{k}s} \langle |\psi_{\mathbf{k}}(\mathbf{R}_j)| m_s f(\mathbf{k},s)\rangle_P, \quad (3.16)$$

where s is the electron spin, m_s is the spin, $\mathbf{R}_j$ is the position of the jth atom, and $f(\mathbf{k},s)$ is the Fermi function. $|\psi_{\mathbf{k}}(\mathbf{R}_j)|^2$ is easily simplified

$$|\psi_{\mathbf{k}}(\mathbf{R}_j)|^2 = |\phi_{\mathbf{k}}'(\mathbf{R}_j) - \sum_t \Theta_t(0)\langle\Theta_t(\mathbf{r}-\mathbf{R}_j)|\phi_{\mathbf{k}}'\rangle|^2/\langle\psi_{\mathbf{k}}|\psi_{\mathbf{k}}\rangle = |\sum_{\mathbf{G}} \beta_{\mathbf{G}+\mathbf{k}} e^{i(\mathbf{k}+\mathbf{G})\cdot\mathbf{R}_j}|^2, \quad (3.17)$$

where

$$\beta_{\mathbf{G}+\mathbf{k}} = \alpha_{\mathbf{G}+\mathbf{k}}[1 - \sum_t \Theta_t(0)\langle\Theta_t|\mathbf{G}+\mathbf{k}\rangle]/\langle\psi_{\mathbf{k}}|\psi_{\mathbf{k}}\rangle.$$

Since the Fourier transform $\langle\Theta_t|\mathbf{G}+\mathbf{k}\rangle$ of a core s state is a slowly varying function of $|\mathbf{G}+\mathbf{k}|$ and mostly $\mathbf{G}+\mathbf{k}$'s of magnitudes near the Fermi wave vector are mixed, $\beta_{\mathbf{G}+\mathbf{k}}$ may be approximated by

$$\beta_{\mathbf{G}+\mathbf{k}} = C\alpha_{\mathbf{G}+\mathbf{k}},$$

where

$$C = [1 - \sum_t \Theta_t(0)\langle\Theta_t|\mathbf{k}_F\rangle]/\langle\psi_{\mathbf{k}}|\psi_{\mathbf{k}}\rangle, \quad (3.18)$$

$$|\psi_{\mathbf{k}}(\mathbf{R}_j)|^2 = C^2|\phi_{\mathbf{k}}'(\mathbf{R}_j)|^2.$$

Returning to Eq. (3.16), we see that the problem is reduced to one of calculating the ensemble average of

$$\langle |\psi_{\mathbf{k}}(\mathbf{R}_j)|^2 f(\mathbf{k},s)\rangle_P = C^2\langle |\phi_{\mathbf{k}}(\mathbf{R}_j)|^2 f(\mathbf{k},s)\rangle_P. \quad (3.19)$$

We have made at this stage one further assumption, namely, that the density of states at the Fermi energy E_F and the character of the electronic states at E_F are weakly varying functions within the ensemble and can be taken out of the average and replaced by their ensemble average value. Then in (3.19) it is possible to replace the P average of the product by the product of the P averages. This assumption permits us also, at a later stage in the calculation, to change the order of averaging over the ensemble and over the Fermi surface. We therefore write

$$\langle |\phi_{\mathbf{k}}'(\mathbf{R}_j)|^2 f(\mathbf{k},s)\rangle_P = \langle |\phi_{\mathbf{k}}'(\mathbf{R}_j)|^2\rangle_P \langle f(\mathbf{k},s)\rangle_P. \quad (3.20)$$

For a general point in the Brillouin zone, nondegenerate perturbation theory gives

$$\phi_{\mathbf{k}}' = |\mathbf{k}\rangle + \sum_{\mathbf{k}'}{}' \frac{\langle\mathbf{k}'|V_{\text{eff}}|\mathbf{k}\rangle}{E_{\mathbf{k}}^0 - E_{\mathbf{k}'}^0}|\mathbf{k}'\rangle,$$

where $|\mathbf{k}\rangle$ is a plane-wave state.

Proceeding exactly as in the calculation of $\langle E_{\mathbf{k}}(\{\mathbf{R}_\nu\})\rangle_P$, we obtain

$$\langle |\phi_{\mathbf{k}}'(\mathbf{R}_j)|^2\rangle_P = \frac{1}{dNV_0}\Big\{1 + 2\sum_{\mathbf{k}'} \frac{(\mathbf{k}', v_{\text{eff}}\mathbf{k})}{E_{\mathbf{k}}^0 - E_{\mathbf{k}'}^0} \times \Big|\frac{1}{d}\sum_b e^{i\mathbf{G}\cdot\mathbf{R}_b^0} e^{-W}\Big|^2 \delta_{\mathbf{k}-\mathbf{k}',\mathbf{G}} + 2\sum_{\mathbf{k}'} \frac{h(2\bar{n}_{\mathbf{q}s}+1)}{2MN\omega_{\mathbf{q}s}} \frac{(\mathbf{k}', v_{\text{eff}}\mathbf{k})}{(E_{\mathbf{k}'} - E_{\mathbf{k}'}^0)} \Big|\frac{1}{d}\sum_b e^{i\mathbf{G}\cdot\mathbf{R}_b^0} e^{-W}\Big| \times |(\mathbf{k}-\mathbf{k}')\cdot e_{\mathbf{q}sb}|^2 \delta_{\mathbf{k}'\mathbf{k}\pm\mathbf{q}\cdot\mathbf{G}} + \text{higher-order terms in } V_{\text{eff}}\Big\}. \quad (3.21)$$

The third term is much smaller than the second term[21] and is therefore ignored. With this approximation, the result in (3.21) can also be obtained with the ensemble average pseudo-wave-function $\bar{\phi}_{\mathbf{k}}$. Consequently, we have

$$\langle |\phi_{\mathbf{k}}'(\mathbf{R}_j)|^2\rangle_P = \langle |\bar{\phi}_{\mathbf{k}}(\mathbf{R}_j)|^2\rangle_P.$$

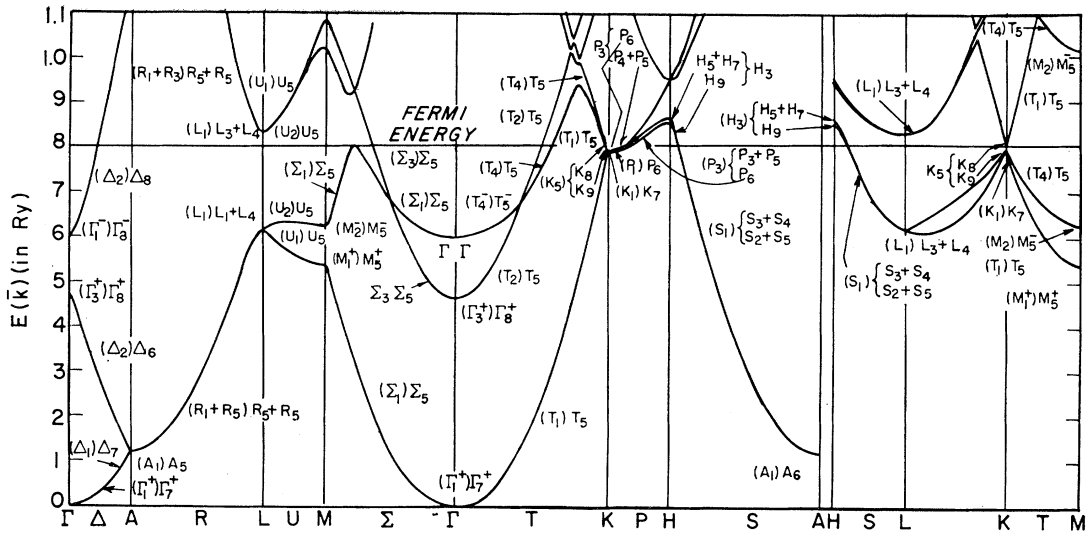

FIG. 1. Band structure of Cd at $T=0°K$.

This means that the ensemble average of $|\phi_{\mathbf{k}}'(\mathbf{R}_j)|^2$ can be calculated by computing the ensemble average of $|\bar{\phi}_{\mathbf{k}}(\mathbf{R}_j)|^2$. In other words, in each member of the ensemble the function $\phi_{\mathbf{k}}$ changes as well as the point $\mathbf{R}_j$ where it has to be measured; it is equivalent to the order of accuracy we desire to take one function, namely $\bar{\phi}_{\mathbf{k}}$, and calculate the average over the different values $\mathbf{R}_j$, the point where that function is evaluated.

It is now easily found[7] with the above assumptions that

$$K_{\text{iso}}\cong(8\pi/3)\langle\chi_p\rangle_P C^2\langle\langle|\bar{\phi}_{\mathbf{k}}(\mathbf{R}_j)|^2\rangle_P\rangle_F, \quad (3.22)$$

where $\langle\chi_p\rangle_P$ is the ensemble-average Pauli-spin susceptibility.

A similar derivation for K_{an} yields

$$K_{\text{an}}=3\langle\chi_p\rangle_P\langle\langle\bar{\psi}_{\mathbf{k}}|(3\cos^2\alpha-1)/r^3|\bar{\psi}_{\mathbf{k}}\rangle\rangle_P\rangle_F, \quad (3.23)$$

where $\bar{\psi}_{\mathbf{k}}$ is defined by

$$\bar{\psi}_{\mathbf{k}}=\bar{\phi}_{\mathbf{k}}-\sum_{tj}\Theta_t(\mathbf{r}-\mathbf{R}_j)\langle\Theta_t(\mathbf{r}-\mathbf{R}_j)|\bar{\phi}_{\mathbf{k}}\rangle \quad (3.24)$$

and α is the angle between the applied field and the radius vector $\mathbf{r}$ from the nuclear site to the electron.

IV. PP AND ENERGY BANDS

The PP used is that of SF except for the two differences already discussed: (1) The ions are allowed to vibrate about their equilibrium positions, and (2) the volume per atom and the reciprocal-lattice vectors are changed with temperature to agree with the experimental lattice constants at that particular temperature.[22]

The form of the empirical PP is

$$V_{\text{eff}}=V_{\text{L}}+V_{\text{N}}+W_{\text{so}},$$

where V_{L}, V_{N}, and W_{so} are the local potential, the nonlocal potential, and the spin-orbit interaction, respectively. The components of V_{eff} have the following forms:

(a) Local potential

$$V_{\text{L}}(\mathbf{r},\{\mathbf{R}_j\})=\sum_{hj}U_{\text{L}}(\mathbf{G}_h)e^{i\mathbf{G}_h\cdot(\mathbf{r}-\mathbf{R}_j)},$$

where $U_{\text{L}}(\mathbf{G}_h)$ has been fitted to experiment[9] and is taken to be nonzero for the $\{0002\}$, $\{10\bar{1}0\}$, $\{10\bar{1}1\}$, and $\{10\bar{1}2\}$ reciprocal-lattice vectors in the hexagonal Brillouin zone; $\mathbf{R}_j$ labels the atomic sites which are displaced from their equilibrium positions.

(b) Nonlocal potential

$$V_{\text{N}}=\sum_{tj}v(t)|\Theta_t(\mathbf{r}-\mathbf{R}_j)\rangle\langle\Theta_t(\mathbf{r}-\mathbf{R}_j)|,$$

where the index t runs over the s, p, and d states of the outermost occupied core shell. The functions $|\Theta_t(\mathbf{r}-\mathbf{R}_j)\rangle$ are the Hartree-Fock-Slater atomic functions centered at the atomic sites $\mathbf{R}_j$, and the $v(t)$ are once again parameters determined by SF to fit experimental data.

(c) Spin-orbit term

$$W_{\text{so}}(\mathbf{k},s,\mathbf{k}',s')=i[\lambda_p+\lambda_d(\mathbf{k}\cdot\mathbf{k}')]\mathbf{k}'\times\mathbf{k}\cdot\boldsymbol{\sigma}_{ss'},$$

where $\boldsymbol{\sigma}_{ss'}$ are the s, s' components of the Pauli matrices.

The smooth pseudo-wave-function $\bar{\phi}_{n\mathbf{k}}$

$$\bar{\phi}_{n\mathbf{k}}=\sum_{\mathbf{G}}\alpha_{\mathbf{G}+\mathbf{k}}|\mathbf{G}+\mathbf{k}\rangle \quad (4.1)$$

satisfies the PP wave equation

$$(\mathbf{p}^2/2m+V_{\text{L}}+V_{\text{N}}+W_{\text{so}})\bar{\phi}_{n\mathbf{k}}=E_{n\mathbf{k}}\bar{\phi}_{n\mathbf{k}},$$

where n and $\mathbf{k}$ denote the band index and wave vector.

[22] $T=0°K$—Ref. 9; $T=298°K$—E. R. Jette and F. Foote, J. Chem. Phys. **3**, 605 (1935); $T=462°K$—J. F. Kossolapow and A. K. Trapesnikow, Z. Krist. **91A**, 410 (1935).

The PP parameters chosen by SF are shown in Table I.[9] The low-temperature band structures resulting from these parameters are displayed in Fig. 1. These band structures show a significant departure from a nearly-free-electron hcp band structure.[18,23] The so-called butterflies (third and fourth bands centered about L) are raised above the Fermi level, and the monster (second-band hole surface) is not connected across the ΓM symmetry line. These differences result from the large, nonlocal contribution to the PP from the outer d shells of the ion cores.

Spin-orbit coupling does not affect the bands significantly, and it has not been included in the form of the PP used to calculate the Knight shift here; i.e., we have made $\lambda_p=\lambda_d=0$.

Now we examine the energy bands and Fermi surface at higher temperatures, i.e., $T=298$, 462°K. The band structures are calculated in a manner similar to that of SF, except that the lattice parameters are changed[22] and the structure factor

$$S_{T=0°\mathrm{K}}(\mathbf{G})=\cos 2\pi[\tfrac{1}{6}(h+2k)+\tfrac{1}{4}l]$$

is replaced by

$$S_T(\mathbf{G})=e^{-W(\mathbf{G},T)}\cos 2\pi[\tfrac{1}{6}(h+2k)+\tfrac{1}{4}l]. \quad (4.2)$$

We must then evaluate $W(\mathbf{G},T)$

$$W(\mathbf{G},T)=\tfrac{1}{2}\sum_{qs}(\hbar/2MN\omega_{qs})(2\bar{n}_{qs}+1)\,|\,(\mathbf{G}\cdot\mathbf{e}_{qsb})\,|^2,$$

which we approximate by

$$W(\mathbf{G},T)=D(T)\mathbf{G}^2,$$

with

$$D(T)=\frac{1}{6}\frac{2NV_0}{(2\pi)^3}\int d\mathbf{q}\left(\frac{\hbar}{2MN\omega_{qs}}\right)(2\bar{n}_{qs}+1).$$

The phonon dispersion relations used to calculate $D(T)$ are those extrapolated from Zn.[11] The results are

$$D(T=0°\mathrm{K})=0.004,\quad D(T=298°\mathrm{K})=0.093,$$
$$D(T=462°\mathrm{K})=0.150.$$

The accuracy of quantitative calculations using this temperature-dependent band structure is sensitive to the choice of phonon dispersion curves.

TABLE I. Temperature-dependent parameters of the band calculations.

T (°K)	Crystal structure parameters a (Å)	c (Å)	Debye factor $D(T)$ (Bohr radii)$^{-2}$	Fermi energy E_F (Ry)
0	2.9684	5.5261	0.004	0.651
298	2.973	5.606	0.093	0.644
462	2.984	5.650	0.110	0.634

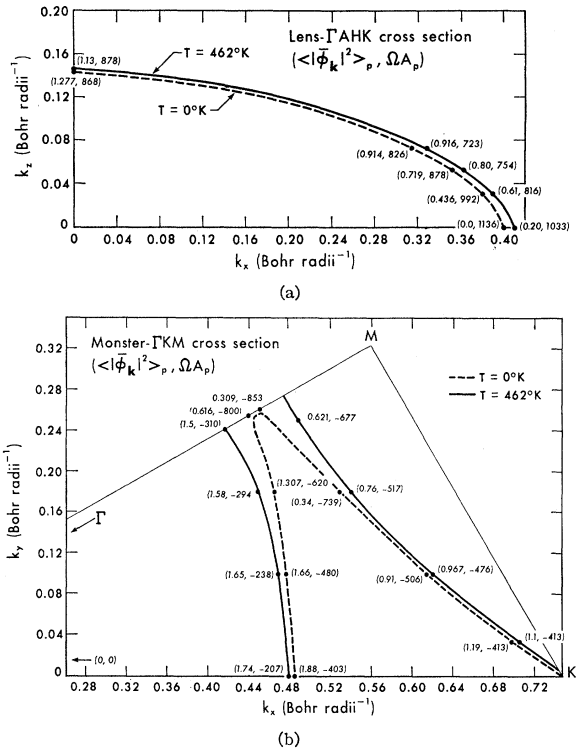

FIG. 2. Comparison of cross sections of the Fermi surface of Cd at $T=0$ and $T=462$°K, along with the values of $\langle|\bar{\phi}_\mathbf{k}|^2\rangle_p$ and A_p for various points on the Fermi surfaces. (a) Cross section of the lens in the ΓAHK plane. (b) Cross section of the monster in the ΓKM plane ($Z=0.0$).

Figure 2 shows the resultant Fermi surfaces at $T=0$ and $T=462$°K. The Fermi surface at $T=462$°K becomes more free-electron-like in that the waist connects across the ΓM line and the butterfly drops below the Fermi level. These have a large effect on the spin susceptibility and the Knight shift, which we calculate in Sec. V.

V. CALCULATION OF SPIN SUSCEPTIBILITY AND KNIGHT SHIFT

A. Calculation of $\chi_p(T)$

The spin susceptibility for a gas of noninteracting electrons is

$$\chi_p=\mu_0^2N(E_F), \quad (5.1)$$

where $N(E_F)$ is the density of states at the Fermi surface and μ_0 is the Bohr magnetism. The susceptibility for a real metal can be quite different from the free-electron gas because of the electron-electron interaction. Pines[24] has shown that the electron-electron interaction enhances the spin susceptibility, with the enhancement being primarily a function of the electron density. The enhancement factor has not been calculated for Cd.

[23] J. C. Slater, *Quantum Theory of Molecules and Solids* (McGraw-Hill Book Co., New York, 1965), Vol. II, p. 467.

[24] David Pines, in *Solid State Physics*, edited by F. Seitz and D. Turnbull (Academic Press Inc., New York, 1955), Vol. I, p. 367.

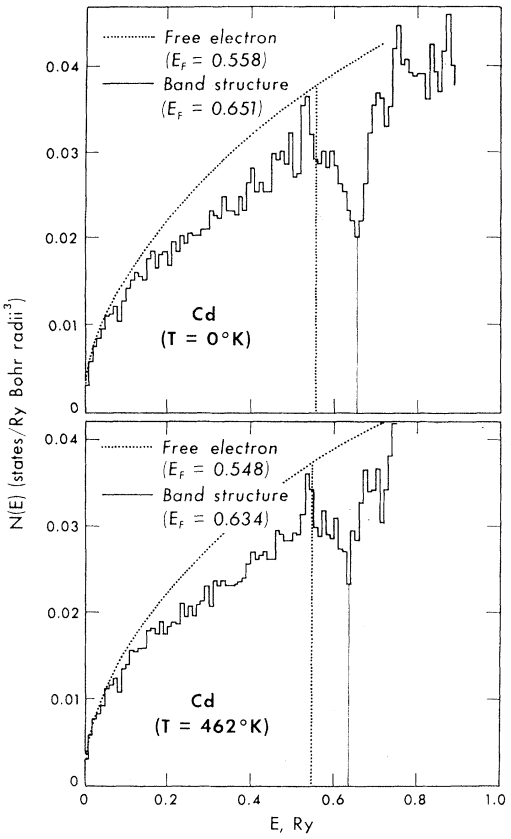

FIG. 3. Density-of-states curves for Cd at $T=0$ and $T=462$°K. Corresponding free-electron curves and Fermi energies are also shown.

However, we have estimated it by fitting our calculated $K_{\rm iso}$ at $T=0$°K to the experimental value. The same enhancement factor is then used for $K_{\rm an}$ at $T=0$°K and for both $K_{\rm iso}$ and $K_{\rm an}$ at the other temperatures. This enhancement turns out to be 1.55.

Assuming (5.1) to be correct, we need only calculate the density of states at the Fermi surface. The density of states $N(E_F)$ refers to the band density of states and is obtained from the band structure.[25]

The density of states was calculated at the three temperatures $T=0$, 298, and 462°K. For $T=0$ and $T=462$°K, eigenvalues were calculated on a mesh of 200 points in a 1/24 symmetry section of the Brillouin zone. The number of mesh points being too small for reliable statistics in a 0.01-Ry spectral histogram of $N(E)$, a Monte Carlo routine was used to generate 15 030 points in the Brillouin-zone symmetry section. The corresponding eigenvalues at these points were obtained by quadratic interpolation and then placed in their proper spectral boxes. The resulting curves for $N(E)$ are shown in Fig. 3.

[25] The density of states as obtained from electronic specific-heat data contains an electron-phonon interaction enhancement factor. That correction does not apply in the calculation of χ_p.

The Fermi energies are $E_F(T=0°\text{K})=0.651$ Ry and $E_F(T=462°\text{K})=0.634$ Ry. The density of states at $T=462$°K is 16% greater than that at $T=0$°K. It should also be pointed out that the density of states at the Fermi energy for $T=0$°K agrees excellently with the experimental value extracted from superconductivity data,[11] as well as with the specific-heat value when electron-phonon corrections are properly taken into account.

In order to save computation time, the Fermi energy and density of states at $T=298$°K were determined not by a detailed and lengthy numerical calculation as in the other two cases, but by an approximate scheme which consisted of the following steps: (a) estimation of the Fermi energy by averaging the energy shifts at a fairly small ($\cong 30$) number of points close to the Fermi surface, $E_F^{(298°\text{K})}=0.644$ Ry, and (b) averaging over the Fermi surface the change in electron group velocities $|\nabla_{\mathbf{k}}E|$.

The density of states at $T=298$°K was found to be 10% larger than the $T=0$°K value.

This yields, from (5.1), the susceptibility (in cgs volume units)

$$\chi_p(T=0°\text{K})=0.54\times10^{-6},$$
$$\langle\chi_p(T=298°\text{K})\rangle_p=0.60\times10^{-6},$$
$$\langle\chi_p(T=462°\text{K})\rangle_p=0.63\times10^{-6}.$$

At $T=0$, the fairly large crystal potential is the cause of the sizable decrease in density of states at E_F from the corresponding free-electron value (see Fig. 3). At higher temperatures the factor $e^{-W(\mathbf{k},T)}$ effectively reduces the potential $V_{\rm eff}$ and allows the density of states to become closer to the free-electron value. In the limit of vanishing potential ($V_{\rm eff}\to 0$) one could obtain once again the free-electron density of states.

One can see this effect more explicitly by looking at the Fermi surface. It becomes increasingly free-electron-like at higher temperatures. Figure 2 shows this effect for the lens and the monster.

B. Calculation of $K_{\rm iso}$

In Sec. 3, we showed that

$$K_{\rm iso}\cong(8\pi/3)\langle\chi_P(T)\rangle_P C^2\langle\langle|\tilde{\phi}_{\mathbf{k}}(\mathbf{R}_j)|^2\rangle_P\rangle_F,$$

where $C^2=669$ (evaluated by using the wave functions given by Herman and Skillman[26]).

By means of (4.1) we obtain

$$\langle|\tilde{\phi}_{\mathbf{k}}(\mathbf{R}_j)|^2\rangle_P=\sum_{\mathbf{G}}\frac{\alpha_{\mathbf{G}+\mathbf{k}}^2}{2NV_0}+\frac{1}{2NV_0}\sum_{\mathbf{G}'\neq\mathbf{G}}\alpha_{\mathbf{G}+\mathbf{k}}\alpha_{\mathbf{G}'+\mathbf{k}}S(\mathbf{G}-\mathbf{G}'),\quad(5.2)$$

[26] F. Herman and S. Skillman, *Atomic Structure Calculations* (Prentice-Hall, Inc., Englewood Cliffs, N. J., 1965).

where $S(\mathbf{G}-\mathbf{G}')$ is the structure factor (4.2) and n is the order of the secular equation.

The average density of the electron in state $\mathbf{k}$ at the nuclear position $(\langle|\tilde{\phi}_{\mathbf{k}}(\mathbf{R}_j)|^2\rangle_p)$ has a wide range of values for states on different regions of the Fermi surface (see Fig. 2). A Fermi-surface average of this density therefore requires calculation at many points.

For each of the three temperatures ($T=0$, 298, 462°K), we calculated the electron density for 34 points on the monster and for nine points on the lens. The lens was approximated by an oblate ellipsoid of revolution, thus enabling an accurate Fermi-surface average over it to be performed. The average over the monster part of the Fermi surface was performed by dividing it into strips, the boundaries of the strips being planes parallel to the [0001] axis. The most troublesome surfaces here are the sharply rounded corners (see Fig. 2), where the density varies greatly; however, only small errors should result, since the density is smallest here.

Putting together the two averages above, we found

$$\begin{aligned}\Omega_0\langle\langle|\tilde{\phi}_k|^2\rangle_p\rangle_F&=0.74, \quad \text{at} \quad T=0°\text{K}\\ &=0.81, \quad \text{at} \quad T=298°\text{K}\\ &=0.86, \quad \text{at} \quad T=462°\text{K}\end{aligned}$$

where Ω_0 is the crystal volume.

Thus, relative to the $T=0$°K density, the density at 298 and 462°K increased by 9 and 15%, respectively. The large part of this increase resulted from a change of the wave functions in the monster from p to s character.

Using $\langle\chi_p\rangle_P$ from the previous section, along with the enhancement factor of 1.55, we find close agreement with experiment, as is shown in Fig. 4. K_{iso} increases by 19% at $T=298$°K and by 31% at $T=462$°K:

$$K_{\text{iso}}(0°\text{K})=0.35, \quad K_{\text{iso}}(298°\text{K})=0.42,$$
$$K_{\text{iso}}(462°\text{K})=0.47.$$

We can also investigate whether the NMR of Cd above its melting point can be well approximated by that of an interacting free-electron gas.[27] The electron density at a nucleus should be

$$\Omega_0\langle\langle|\tilde{\phi}_{\mathbf{k}}|^2\rangle_P\rangle_F=1.0,$$

and the density of states is the free-electron density of states giving

$$\langle\chi_p\rangle_P=(1/0.57)\chi_p(T=0°\text{K}).$$

We then obtain

$$K_{\text{iso}}=0.81\%.$$

This compares excellently with the experimental value of 0.80%.

Thus our calculation of K_{iso} fits experiment closely. Core-polarization and orbitals effects are probably small, in agreement with Dickson's prediction based on experiment.[15]

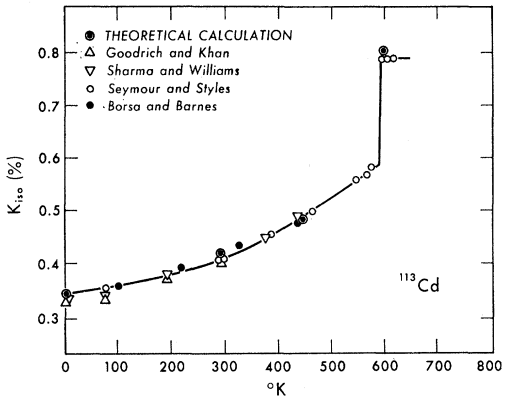

FIG. 4. Experimental and theoretical isotropic Knight shift.

C. Calculation of K_{an}

The anisotropic Knight shift K_{an} is given by Eqs. (3.24) and (3.25). In order to evaluate K_{an} we must evaluate the matrix element of $P_2(\cos\alpha)$. When the PP form is used [Eq. (3.25)], many terms appear. The dominant terms (an order of magnitude larger than the others) are the two which involve matrix elements of $P_2(\cos\alpha)$ between core wave functions and between core wave functions and plane waves. When in addition selection rules for matrix elements of spherical harmonics are used, the relevant matrix elements can be expressed as

$$\langle\langle\tilde{\psi}_{\mathbf{k}}|(3\cos^2\alpha-1)/r^3|\tilde{\psi}_{\mathbf{k}}\rangle\rangle_P=A_p+A_{sd}, \qquad (5.3)$$

where

$$A_p=\sum_{\mathbf{G}'}\sum_{\mathbf{G}}\alpha_{\mathbf{G}'+\mathbf{k}}\alpha_{\mathbf{G}+\mathbf{k}}S(\mathbf{G}-\mathbf{G}')\sum_m\langle\mathbf{G}'+\mathbf{k}|\Theta_{4pm}\rangle$$
$$\times\langle\Theta_{4pm}|(3\cos^2\alpha-1)/r^3|\Theta_{4pm}\rangle\langle\Theta_{4pm}|\mathbf{G}+\mathbf{k}\rangle,$$
$$A_{sd}=\sum_{\mathbf{G}'}\sum_{\mathbf{G}}\alpha_{\mathbf{G}'+\mathbf{k}}\alpha_{\mathbf{G}+\mathbf{k}}S(\mathbf{G}-\mathbf{G}')(8\pi/5)$$
$$\times\sum_m\{\langle\mathbf{G}'+\mathbf{k}|\Theta_{4dm}\rangle\langle\Theta_{4dm}|(3\cos^2\alpha-1)/r^3|\mathbf{G}+\mathbf{k}\rangle$$
$$+\langle\mathbf{G}'+\mathbf{k}|(3\cos^2\alpha-1)/r^3|\Theta_{4dm}\rangle\langle\Theta_{4dm}|\mathbf{G}+\mathbf{k}\rangle\}.$$

The value of A_{sd} was calculated at the three temperatures and was found to be

$$\Omega_0A_{sd}(0°\text{K})=21, \quad \Omega_0A_{sd}(298°\text{K})=24,$$
$$\Omega_0A_{sd}(462°\text{K})=22.$$

It is apparent from these values that it is temperature-independent to a very good approximation. It is also positive, with positive contributions from the lens and monster and, as will be seen immediately, is only about 20% of the absolute value of A_p.

[27] N. C. Halder, Phys. Rev. **177**, 471 (1968). Halder's results suggest that the free-electron approximation may not be valid for liquid metals.

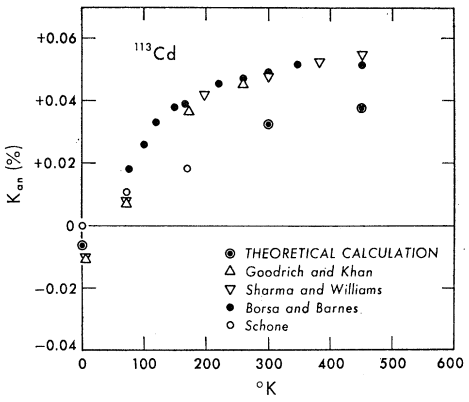

FIG. 5. Experimental and theoretical anisotropic Knight shift.

The quantity A_p in Eq. (5.3) as calculated by the methods of Sec. V B yields

$$\Omega_0 A_p(0°\mathrm{K}) = -44, \quad \Omega_0 A_p(298°\mathrm{K}) = 99,$$
$$\Omega_0 A_p(462°\mathrm{K}) = 104.$$

When these values are replaced in Eq. (5.3) along with A_{sd}, we obtain

$$K_{an}(0°\mathrm{K}) = -0.006\%, \quad K_{an}(298°\mathrm{K}) = 0.034\%,$$
$$K_{an}(462°\mathrm{K}) = 0.037\%.$$

These values and the experimental curves are displayed in Fig. 5. The discrepancy could be calculational since A_p has its largest values in the highly rounded regions of the monster (see Fig. 2)

The values of A_p deserve some separate remarks. The contribution to A_p from the lens is of positive sign (i.e., functions with p_z-like summetry) while the contribution from the monster is negative, indicating p_x-p_y-like symmetry. The contributions from both parts, then, tend to cancel one another, and almost complete cancellation occurs at $T=0°\mathrm{K}$. As the temperature increases, several changes take place: (1) The s-p character of the wave functions on the lens changes only very slightly; (2) the s character of the wave functions on the monster increases sizably at the expense of the p part, diminishing the contribution of the negative p_x-p_y part of A_p; (3) the Fermi-surface area of the monster increases more rapidly than that of the lens, contributing to an increase of the negative part of A_p; and (4) the butterfly gives also a negative contribution at those temperatures for which the corresponding level falls below the Fermi energy.

As a consequence of these four changes, K_{an} first increases with temperature because of (1) and (2) and then tends to saturation as a result of (3) and (4).

VI. CONCLUSIONS

By including the effect of lattice vibrations in the PP scheme of calculating electronic properties of metals, we have explained the apparently paradoxical result of the changes in the isotropic and anisotropic parts of the Knight shift.

Qualitatively, all effects can be explained in terms of the following simple theoretical results: (1) The third-band lens is a mixture of s-like and p_z-like states, which are moreover, roughly temperature-independent; (2) the second-zone-hole monster consists mostly of states which in the neighborhood of the ions are s-like and p_x-p_y-like; (3) the shape and symmetry of the states on the second-zone surface are very sensitive to the strength and symmetry of the PP; and (4) as the temperature increases and the PP decreases in strength and becomes less anisotropic, the states on the second-zone monster become more s-like and less p_x-p_y-like.

As a consequence of these four effects we find that (a) as the temperature increases, the s contribution of the monster increases, with a consequent increase in K_{iso}. (b) As the temperature increases, the p_x-p_y contribution of the monster decreases, with a consequent destruction of the almost exact cancellation between p_x-p_y contribution of the monster and p_z contribution of the third-zone lens; K_{an} therefore also increases. (c) Upon melting, Cd becomes a free-electron-like metal and K_{iso} increases by 33%. This agrees with Ziman's hypothesis[28] and confirms it quantitatively.

In conclusion, we would like to point out that the effect found in Cd and not in most other metals (Mg with equal valence and structure shows a temperature-independent Knight shift[29]), should also appear in Zn, which has a very similar electronic structure and PP. If the serious difficulties which arise from the low isotropic abundance of Zn^{67} and the poor signal-to-noise ratio in the NMR signal could be overcome, experimental confirmation of this hypothesis should prove quite interesting. In addition, Zn and Cd should both exhibit strongly temperature-dependent properties in other experimental data, in particular in the optical spectra. A theoretical study of this effect is now under way.

ACKNOWLEDGMENTS

It gives me great pleasure to thank Professor L. M. Falicov for suggesting this problem and for his invaluable guidance and encouragement. I would also like to thank Dr. J. C. Kimball for many helpful discussions. I am grateful to Professor A. Bienenstock for a copy of the unpublished thesis of S. C. Yu (Harvard University, 1964). I would also like to thank Dr. Edward Mark Dickson for a copy of his thesis [Nuclear Magnetic Resonance in Cadmium and Tin, University of California at Berkeley, 1968 (unpublished)] which proved extremely useful, and for pointing out his estimate of core polarization and orbital effects on K_{iso}. I wish to thank the University of California at Berkeley

[28] J. M. Ziman, Advan. Phys. **16**, 421 (1967).
[29] P. D. Dougan, S. N. Sharma, and D. Llewelyn Williams (to be published).

for its hospitality and services provided during the final stages of this work. A predoctoral fellowship from the National Science Foundation, which I held throughout my graduate career, is gratefully acknowledged. This work has been directly supported by the National Science Foundation and the Office of Naval Research. In addition it has benefited from general support to the Material Sciences at the University of Chicago by the Advanced Research Projects Agency.

APPENDIX

Consider the equation

$$\langle e^{i\mathbf{k}\cdot\mathbf{y}_\nu}e^{i\mathbf{k}\cdot\mathbf{y}_\mu}\rangle_p=1+\langle\tfrac{1}{2}[(i\mathbf{k}\cdot\mathbf{y}_\nu)(i\mathbf{k}\cdot\mathbf{y}_\mu)]^2\rangle_p+\cdots. \quad \text{(A1)}$$

The terms with an odd number of factors of $\mathbf{y}$ go to zero because they contain products of an odd number of creation and/or destruction operators.

Since $\langle i\mathbf{k}\cdot\mathbf{y}_\nu\rangle_p$ is small compared to unity, (A1) can be written as

$$\langle e^{i\mathbf{k}\cdot\mathbf{y}_\nu}e^{i\mathbf{k}\cdot\mathbf{y}_\mu}\rangle_p=e^{-W}e^{-W'}e^{\frac{1}{2}(i\mathbf{k}\cdot\mathbf{y}_\mu i\mathbf{k}\cdot\mathbf{y}_\nu+i\mathbf{k}\cdot\mathbf{y}_\nu i\mathbf{k}\cdot\mathbf{y}_\mu)}$$
$$=e^{-W}e^{-W'}+e^{-W}e^{-W'}\times\tfrac{1}{2}\langle i\mathbf{k}\cdot\mathbf{y}_\mu i\mathbf{k}\cdot\mathbf{y}_\nu+i\mathbf{k}\cdot\mathbf{y}_\nu i\mathbf{k}\cdot\mathbf{y}_\mu\rangle_p,$$

where W refers to the νth atom and W' refers to the μth atom.

Equation (3.8) and the properties of creation and destruction operators give

$$\tfrac{1}{2}\langle i\mathbf{k}\cdot\mathbf{y}_\mu i\mathbf{k}\cdot\mathbf{y}_\nu+i\mathbf{k}\cdot\mathbf{y}_\nu i\mathbf{k}\cdot\mathbf{y}_\mu\rangle=\sum_{\mathbf{q}s}(\hbar/2MN\omega_{\mathbf{q}s})$$
$$\times\{[\mathbf{k}\cdot\mathbf{e}_{\mathbf{q}sb}][\mathbf{k}\cdot\mathbf{e}_{\mathbf{q}sb'}](\bar{n}_{\mathbf{q}s}+1)e^{i\mathbf{q}\cdot(\mathbf{R}_\nu{}^0-\mathbf{R}_\mu{}^0)}+\text{c.c.}\}. \quad \text{(A2)}$$

PHYSICAL REVIEW VOLUME 187, NUMBER 3 15 NOVEMBER 1969

Phase-Shift Analysis of the Fermi Surface of Copper

MARTIN J. G. LEE
The James Franck Institute and Department of Physics, The University of Chicago, Chicago, Illinois 60637

(Received 17 April 1969)

In an earlier paper a method was described whereby the partial-wave phase shifts that characterize the interaction between the conduction electrons and the lattice in a metal may be derived from experimental Fermi-surface data. In the present paper we apply the method of phase-shift analysis to study the shape of the Fermi surface of copper, which is known to be strongly perturbed by the *d*-like energy bands that lie almost 2 eV below the Fermi level. By adjusting the values of the *s*, *p*, *d*, and *f* phase shifts, and the Fermi-energy parameter, we construct a model Fermi surface on which the areas of the ⟨100⟩ belly and the ⟨111⟩ neck and belly orbits, the dog's bone, the four-cornered rosette, and the lemon orbit, are in good agreement with the results of precision measurements of the corresponding de Haas–van Alphen frequencies. The belly anisotropy of the model surface is also in good agreement with the experimental data, and the volume enclosed by the surface does not differ significantly from 1 electron/atom. The radii of the Fermi surface of copper in the (100) and (110) symmetry zones are determined to an accuracy of ±0.1%, and the results are in good agreement with the radii recently deduced by Halse by an independent technique. It is shown that the numerical values of the phase shifts are consistent with the position of copper in the Periodic Table. The local potential of Chodorow for Cu^+ produces phase shifts that are in substantial agreement with the results of the present work. A simple nonlocal correction to the Chodorow potential is proposed, such that the Fermi surface derived from the modified potential is entirely consistent with the experimental data. The energies associated with certain optical transitions in metallic copper are computed from the modified potential, and are found to agree with the results of recent piezo-optical experiments to better than 0.2 eV. It is concluded that the method of phase-shift analysis is capable of representing accurately the form of the *d*-like electronic energy bands in metals, and that the modified Chodorow potential may well prove to be the best starting point for a full calculation of the band structure of copper in the vicinity of the Fermi level.

I. INTRODUCTION

AS a result of several experimental investigations,[1–9] the geometry of the Fermi surface of copper is now known in substantial detail. Copper crystallizes in a fcc structure, and single crystals of copper may readily be grown with the high degree of chemical and structural perfection necessary for Fermi-surface studies by resonance techniques. According to the free-electron model, one would expect the Fermi surface of copper to be spherical and to lie entirely within the first Brillouin zone, which for the fcc Bravais lattice is a

[1] A. B. Pippard, Phil. Trans. Roy. Soc. (London) **A250**, 325 (1957).
[2] Yu. P. Gaĭdukov, Zh. Eksperim. i Teor. Fiz. **37**, 1281 (1959) [English transl.: Soviet Phys.—JETP **10**, 913 (1960)].
[3] D. Shoenberg, Phil. Trans. Roy. Soc. (London) **A255**, 85 (1962).
[4] H. V. Bohm and V. J. Easterling, Phys. Rev. **128**, 1021 (1962).
[5] A. S. Joseph, A. C. Thorsen, E. Gertner, and L. E. Valby, Phys. Rev. **148**, 569 (1966).
[6] I. M. Templeton, Proc. Roy. Soc. (London) **A292**, 413 (1966).
[7] J.-P. Jan and I. M. Templeton, Phys. Rev. **161**, 556 (1967).
[8] W. J. O'Sullivan and J. E. Schirber, Phys. Rev. **170**, 667 (1968); *ibid.*, Addendum (to be published).
[9] M. R. Halse, thesis, University of Cambridge, 1968 (unpublished); and Phil. Trans. Roy. Soc. (London) **A265**, 507 (1969).